



# Co-reduction of nitrate and perchlorate in a pressurized hydrogenotrophic reactor with complete H<sub>2</sub> utilization

Razi Epsztein\*, Chaitanyakumar Desitti, Michael Beliafski, Sheldon Tarre, Michal Green

Faculty of Civil and Environmental Engineering, Technion – Israel Institute of Technology, Haifa 32000, Israel

## HIGHLIGHTS

- A two-stage hydrogenotrophic process to remove NO<sub>3</sub><sup>-</sup> and ClO<sub>4</sub><sup>-</sup> is presented.
- NO<sub>3</sub><sup>-</sup> is removed in a first unsaturated-flow pressurized reactor stage.
- The residual H<sub>2</sub> is coupled to ClO<sub>4</sub><sup>-</sup> reduction in a second polishing stage.
- Large presence of *Dechloromonas* was detected before and after ClO<sub>4</sub><sup>-</sup> addition.
- Effluent ClO<sub>4</sub><sup>-</sup> concentration of 2 μg/L and ~100% H<sub>2</sub> utilization were achieved.

## ARTICLE INFO

### Article history:

Received 8 April 2017

Received in revised form 26 June 2017

Accepted 29 June 2017

Available online 30 June 2017

### Keywords:

Hydrogenotrophic denitrification

Pressurized reactor

Perchlorate reduction

Hydrogen utilization

Trace concentrations

## ABSTRACT

A novel pressurized hydrogenotrophic reactor operating at high rates was recently developed specifically for the removal of nitrate (NO<sub>3</sub><sup>-</sup>) from drinking water. The reactor is characterized by safe and economical operation since hydrogen (H<sub>2</sub>) purging intrinsic to conventional H<sub>2</sub>-based denitrifying systems is not required and H<sub>2</sub> loss occurs only through the effluent, resulting in H<sub>2</sub> utilization efficiency above 90%. In this research, a new treatment scheme to remove NO<sub>3</sub><sup>-</sup> and perchlorate (ClO<sub>4</sub><sup>-</sup>) combining the pressurized reactor with a following open-to-atmosphere polishing unit is presented. In the pressurized reactor, NO<sub>3</sub><sup>-</sup> and ClO<sub>4</sub><sup>-</sup> are simultaneously removed. In the polishing unit, the residual dissolved H<sub>2</sub> from the pressurized reactor serves to further reduce ClO<sub>4</sub><sup>-</sup> to trace concentrations below recommended levels.

First, ClO<sub>4</sub><sup>-</sup> reduction together with denitrification was demonstrated in the pressurized reactor without special inoculation and a maximal ClO<sub>4</sub><sup>-</sup> volumetric removal rate of 1.83 g/(L<sub>reactor</sub>-d) was achieved. Microbial population analyses before and after the addition of ClO<sub>4</sub><sup>-</sup> were similar with a large fraction of the genus *Dechloromonas*. Results show that the combined treatment scheme consisting of the pressurized reactor and the polishing unit allowed for the reduction of ClO<sub>4</sub><sup>-</sup> concentration down to a minimal value of 2 μg/L with a simultaneous increase of the H<sub>2</sub> utilization efficiency from 95% up to almost 100%.

© 2017 Elsevier B.V. All rights reserved.

## 1. Introduction

Intensive use of nitrogen-based fertilizers and wastes from rockets facilities are the main sources for groundwater contamination by nitrate (NO<sub>3</sub><sup>-</sup>) and perchlorate (ClO<sub>4</sub><sup>-</sup>), respectively [1,2]. Despite the different pollution source, co-occurrence of both ions is common, especially in groundwater close to military bases that house rockets [2]. In some cases, the high ClO<sub>4</sub><sup>-</sup> concentration in the discharge point can lead to migration of ClO<sub>4</sub><sup>-</sup> in groundwater far away from the focus of pollution and mixing with NO<sub>3</sub><sup>-</sup>-contaminated groundwater, as reported in the Ramat Hasharon area in Israel [3]. High ClO<sub>4</sub><sup>-</sup> levels were also detected

in groundwater throughout the U.S., mainly in California, Nevada, Utah, Arizona and other states where rocket and missile production occurs [4]. Also, ammonium perchlorate (NH<sub>3</sub>ClO<sub>4</sub>) occurs naturally in NO<sub>3</sub><sup>-</sup> deposits that are used in some fertilizers [5]. In California, for example, drinking water sources that contain ClO<sub>4</sub><sup>-</sup> was found to have much higher concentrations of NO<sub>3</sub><sup>-</sup> than wells with no measurable ClO<sub>4</sub><sup>-</sup> [6].

The World Health Organization (WHO) standard for NO<sub>3</sub><sup>-</sup>-N is 11.3 mg/L (as nitrogen) [7]. As for ClO<sub>4</sub><sup>-</sup>, standards are more variable and location-dependent. The Environmental Protection Agency (EPA), for example, established an advisory standard of 15 μg/L, but numerous states in the U.S. promulgated enforceable standards for ClO<sub>4</sub><sup>-</sup> in drinking water of only 2 μg/L [2]. Therefore, a comprehensive solution for meeting the drinking water standards determined by the health organizations is required. In the

\* Corresponding author.

E-mail address: [razi.epsztein@yale.edu](mailto:razi.epsztein@yale.edu) (R. Epsztein).

case of  $\text{ClO}_4^-$ , reduction to trace concentrations is needed and therefore much harder to achieve by any treatment technique [8].

Biological denitrification and biological  $\text{ClO}_4^-$  reduction are two processes proved to efficiently reduce  $\text{NO}_3^-$  and  $\text{ClO}_4^-$  concentrations to the permitted thresholds without the production of waste brine [7,9]. Moreover, many perchlorate-reducing bacteria can grow also on  $\text{NO}_3^-$  and therefore a biological denitrification system may be (but not necessarily) effective for  $\text{ClO}_4^-$  reduction [10]. Using  $\text{H}_2$  gas as the electron donor for bacterial growth in both processes is advantageous over the common organic donors (mostly methanol, ethanol and acetate) for drinking water treatment, mainly due to the lower cell yield of autotrophic bacteria reducing reactor clogging, sludge production and post-treatment costs [7,11]. However, supplying  $\text{H}_2$  economically and safely at high transfer rates remains one of the major challenges for the successful application of  $\text{H}_2$ -based systems [7].

Several hydrogenotrophic systems for removal of  $\text{NO}_3^-$  [12–16],  $\text{ClO}_4^-$  [10,17] and both ions together (i.e. simultaneously removal of  $\text{NO}_3^-$  and  $\text{ClO}_4^-$ ) [5,18–22] were proposed in the last 15 years for the treatment of potable water. Among these technologies, the membrane biofilm reactor (MBfR) has gained the most attention due to its safe and economical gas delivery system with close to 100% utilization efficiency of  $\text{H}_2$  gas, and is implemented in full-scale in various groundwater treatment plants in California, USA since 2012 [23]. Membrane fouling and scaling together with difficulties of biomass control are possible drawbacks of a typical MBfR [7].

Recently, a novel unsaturated-flow pressurized reactor for hydrogenotrophic denitrification of groundwater operating at high denitrification rates together with minimal  $\text{H}_2$  loss and low risk was presented. A detailed explanation and description of the reactor was given by Epsztein et al. [24]. Briefly, the reactor is based on the simple concept suggesting that  $\text{N}_2$  gas build-up in a closed-headspace denitrifying system will not occur due to the fact that at steady state a gas-liquid equilibrium is maintained within the reactor according to Henry's law and effluent water carries the excess of  $\text{N}_2$  gas out of the reactor. Since  $\text{N}_2$  reaches equilibrium in the reactor and does not accumulate over time, there is no need for gas purging and the risky and uneconomical  $\text{H}_2$  loss to atmosphere is eliminated. Hydrogen loss is therefore limited only to the dissolved  $\text{H}_2$  in the effluent and  $\text{H}_2$  utilization efficiencies above 92% were achieved [24]. Except for the MBfR, the

biofilm-electrode reactor [14,17] and a system proposed by Rezania et al. [13], there are no reports on such high utilization efficiencies of  $\text{H}_2$  in hydrogenotrophic systems. In the pressurized reactor, high denitrification rates of up to  $7.5 \text{ g NO}_3^- \text{-N}/(\text{L}_{\text{reactor}} \cdot \text{d})$  are ensured by operating the reactor under an unsaturated flow regime where water is recirculated through the  $\text{H}_2$  gas-enriched headspace and trickled over high surface area biofilm carriers [25].

Despite the promising results of the pressurized reactor, achievement of 100%  $\text{H}_2$  utilization efficiency is essential for improving the safety and the economic viability of the process and to prevent a possible regrowth of biomass in the distribution system and ensure a safe drinking product. In the following research work, the simultaneous removal of  $\text{ClO}_4^-$  and  $\text{NO}_3^-$  was investigated in a modified version of the above reactor, i.e., a combined treatment scheme. The combined treatment scheme (Fig. 1) combines the unsaturated-flow pressurized reactor with an up-flow submerged open-to-atmosphere polishing unit. The polishing unit aims to increase  $\text{H}_2$  utilization ( $\sim 100\%$ ) by the consumption of the residual dissolved  $\text{H}_2$  from the pressurized reactor and further reduction of  $\text{ClO}_4^-$  to trace concentrations below recommended levels (between 1 and  $15 \mu\text{g/L}$ ).

## 2. Materials and methods

### 2.1. Experimental setup

A schematic diagram of the combined treatment scheme is illustrated in Fig. 1. The combined treatment scheme included the unsaturated-flow pressurized reactor, i.e., the main reactor unit, combined with a submerged open-to-atmosphere polishing unit to reduce  $\text{ClO}_4^-$  by the residual dissolved  $\text{H}_2$  in the effluent of the main reactor unit. A detailed description of the main reactor unit was given in an earlier publication [24]. Briefly, it comprised of a clear PVC cylindrical reactor 70 cm in height and 10.5 cm in diameter divided into three unequal parts. The top part of the reactor (height 20 cm) served as an empty headspace, the middle part (height 30 cm) was filled with plastic biofilm carriers (total surface area of  $900 \text{ m}^2/\text{m}^3$ , *Aqwise*) and separated by a metal screen from the bottom part (height 20 cm) of the reactor where recirculating

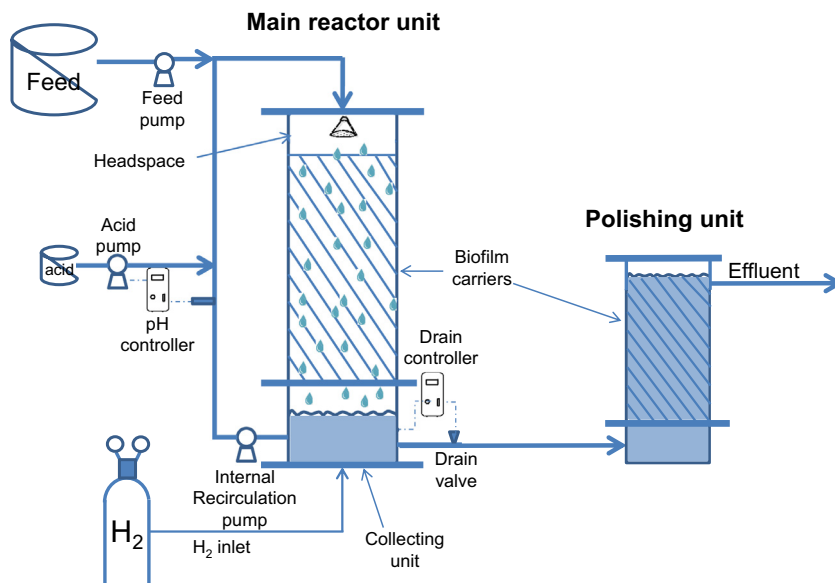


Fig. 1. Schematic diagram of the combined treatment scheme consisting of the unsaturated-flow pressurized reactor, i.e., the main reactor unit, and a following submerged open-to-atmosphere polishing unit.

water collected. Hydrogen gas was supplied continuously from H<sub>2</sub> cylinder. The reactor was connected to a feed pump (Diaphragm pump model 7090-42, Cole-Palmer, USA), recirculation pump (FL-2403, ProPumps, China) and pH controlling unit (standard pH electrode, pH controller – Alpha 190, Eutech, Singapore; hydrochloric acid tank and acid pump – gamma/L, ProMinent, Germany). The main reactor unit was operated as a trickling filter with water recirculation. It was continuously fed with simulated NO<sub>3</sub><sup>-</sup> and ClO<sub>4</sub><sup>-</sup> contaminated groundwater. An automatic drain valve discharged accumulated water to the polishing unit.

The polishing unit comprised of a PVC cylindrical polishing unit 25 cm in height and 10.5 cm in diameter, filled with the same plastic biofilm carriers as in the main reactor unit. The effluent water from the main reactor unit was introduced at the bottom of the polishing unit and released at the top part. The polishing unit was operated under a saturated-flow mode (i.e. submerged unit) and its discharge was open to the atmosphere.

Reactor start-up and initial investigation of ClO<sub>4</sub><sup>-</sup> reduction (Sections 3.1) were performed in the main reactor unit only, using the same biomass carriers from previous denitrification experiments [24]. Start-up of the polishing unit in the following trials was performed by filling the polishing unit with additional clean carriers mixed with biomass carriers from the main reactor unit (the biomass carriers taken from the main reactor unit were replaced with new carriers). Tap water enriched with NaNO<sub>3</sub>, NaClO<sub>4</sub> and KH<sub>2</sub>PO<sub>4</sub> (influent concentration of 1 mg P/L) was used as feed solution for all experiments. Carbon source for bacterial growth was not added and based on the inherent carbon content of the water (alkalinity of ~140 mg/L as CaCO<sub>3</sub> at pH 7.5–8). The recirculation flow rate was 6600 mL/min in the first experiment when only the main reactor unit was used (Section 3.1). In all other trials, the recirculation flow rate in the main reactor unit was 3800 mL/min. Water temperature was kept at 30 ± 1 °C. The pH in the main reactor unit was maintained at 7–7.1 to by dosing hydrochloric acid. The relatively low pH was aimed to prevent an extreme pH increase within the biofilm, which leads to NO<sub>2</sub><sup>-</sup>-N accumulation [26,27]. Samples of influent, effluent from the main reactor unit and effluent from the polishing unit were collected for further water analyses.

Rate calculations in this work were based on the packing volume of the carriers in the main reactor unit (2.5 L) and the polishing unit (1.9 L). In all experiments, excess biomass growth was removed every few days by washing of carriers, column and pipes with tap water (the polishing unit never had to be cleaned).

## 2.2. Water and gas analyses

Nitrate, perchlorate and sulfate were determined using a Metrohm 761 ion chromatograph (IC) equipped with a 150 mm Metrosep A Supp 5 column with column guard and suppressor using a CO<sub>3</sub><sup>2-</sup>/HCO<sub>3</sub><sup>-</sup> eluent. Nitrite-N and alkalinity were measured according to Standard Methods (Method 4500 and Method 2320, respectively). Total Organic Carbon (TOC) concentration was determined by a TOC-VCPH analyzer (Shimadzu, Kyoto, Japan). DOC concentration was determined by performing TOC analysis on samples filtered through 0.22 mm syringe filter. Hydrogen concentration in gas phase was measured by gas chromatography (TCD detector; column: HP-PLOT-Q 30 m; 0.53 mm. 40u, Agilent 7890A). Gas samples were injected directly from the reactor headspace into a 20 mL sealed serum bottle for 1 min with gas flow rate of 250 mL/min to ensure exchange of the entire gas volume in the bottle. Dissolved H<sub>2</sub> concentration was measured by headspace analysis of effluent samples injected to a sealed serum bottle using the same gas chromatograph.

## 2.3. Microbial population analysis using high-throughput sequencing and PCR-DGGE

Biofilm samples for microbial population analysis were taken from the pressurized hydrogenotrophic denitrifying reactor (i.e. the main reactor unit) before (t = 0) and after (t = 25 days) the addition of ClO<sub>4</sub><sup>-</sup>. Total genomic DNA was extracted using FastDNA SPIN Kit for Soil (MP Biomedicals) following the manufacturer's protocol. Pellets of 0.5-mL from suspensions of the reactor's biofilm were used as samples. The DNA concentrations of the extracts were measured with the NanoDrop 1000 Spectrophotometer (Thermo Scientific), adjusted for polymerase chain reaction (PCR) amplification and stored at –20 °C until further use.

High throughput sequencing analysis was performed by using Illumina Miseq (Hy laboratories Ltd, Israel). Samples of DNA were subjected to two rounds of PCR to prepare the libraries for sequencing. The first PCR reaction was performed to amplify the V4 region of the 16 s rDNA gene, with primers that included the CS1 and CS2 sequences from Fluidigm. The second PCR was done using the Access Array Barcode Library for Illumina Sequencers from Fluidigm. The sample data were analyzed using the 16 s metagenomic application on BaseSpace (Illumina). The high quality reads that passed quality filtration were used for the identification of microbial population. Only predominant microbial populations are given; the remaining microbial population is shown as 'Others'.

For DGGE, approximately 600 base pairs (bp) of the 5' end of the variable region V3–V5 of the bacterial 16S rDNA were amplified using the primer pair consisting of 341F (5'-CCTACGGGAGGCAG CAG-3') with a GC clamp (5'-CGCCCGCCGCGCCCGCCCGTCCCG CCGCCCCGCCCCG-3') and 907 R (5'-CCGTCAATTCCTTTRAGTTT-3') [28]. The PCR reactions were performed in a thermocycler (TProfessional Basic Gradient Thermocycler; Biometra) with Apex RED Taq Master Mix (Genesee Scientific Corp.). The PCR conditions, denaturing gradient gel electrophoresis (DGGE) and sequencing procedures were used as mentioned by Desitti et al. [29]. Four dominant bands from DGGE were sequenced and compared with the partial sequence of 16s rDNA bacterial names obtained by high throughput sequencing method. Sequence alignment and phylogenetic tree were performed using MEGA6 [30].

## 3. Results and discussion

### 3.1. Perchlorate removal in the pressurized hydrogenotrophic denitrifying reactor

An initial investigation of ClO<sub>4</sub><sup>-</sup> removal in the pressurized hydrogenotrophic denitrifying reactor using biofilm carriers from former denitrification experiments was first carried out for 25 days. During the experimental period, the inlet NO<sub>3</sub><sup>-</sup>-N and ClO<sub>4</sub><sup>-</sup> concentrations were 15 and 20 mg/L, respectively. The flow rate was increased gradually over time from 20 to 200 mL/min. The reactor's total pressure was 2 bar and the recirculation flow rate was 6600 mL/min. The results for volumetric ClO<sub>4</sub><sup>-</sup> removal rate over time are shown in Fig. 2. Fig. 2 shows that ClO<sub>4</sub><sup>-</sup> reduction started immediately after ClO<sub>4</sub><sup>-</sup> addition, i.e., during the first day of operation. The immediate acclimation of bacteria from the former denitrification reactor to reduce ClO<sub>4</sub><sup>-</sup> demonstrates that no specialized inoculation was required. A maximal ClO<sub>4</sub><sup>-</sup> volumetric removal rate of 1.83 g/(L<sub>reactor</sub>-d) was observed after 25 days of operation. For comparison, Logan et al. reported a slightly lower removal rate of 1.16 g/(L<sub>reactor</sub>-d) in a non-pressurized unsaturated-flow hydrogenotrophic reactor at a lower temperature of 23 °C, similar pH (7) and influent ClO<sub>4</sub><sup>-</sup> concentration (18 mg/L) without NO<sub>3</sub><sup>-</sup> [5]. Sharp fluctuations in the ClO<sub>4</sub><sup>-</sup> removal

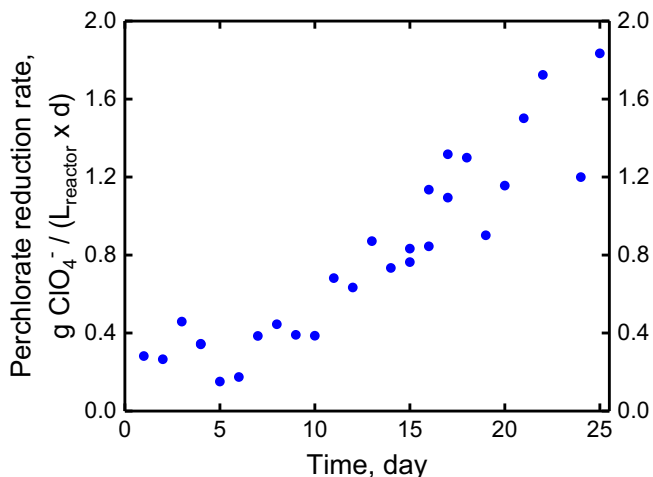


Fig. 2. Volumetric  $\text{ClO}_4^-$  removal rate in the pressurized reactor as a function of time. At  $t = 0$ ,  $\text{ClO}_4^-$  was introduced at the reactor for the first time.

rates (e.g. day 19 and 24) can be attributed to reactor cleaning accompanied with loss of biomass and change of conditions. Effluent  $\text{ClO}_4^-$  concentrations were generally below 1 mg/L (i.e. removal efficiency above 95%), except on days when the loading rate was increased where the effluent concentrations reached 3–4 mg/L  $\text{ClO}_4^-$ . The effluent  $\text{NO}_3^-$ -N concentration from the pressurized reactor was always below 1 mg/L (i.e. removal efficiency above 93%). Effluent  $\text{NO}_2^-$  concentrations were always below detection levels.

### 3.2. Microbial population analysis with high-throughput sequencing and PCR-DGGE

The microbial population was examined before and after the addition of  $\text{ClO}_4^-$  to the pressurized hydrogenotrophic denitrifying reactor (at  $t = 0$  and  $t = 25$  days). Results from high throughput sequencing of the two sampling dates were similar, giving evidence to the presence of bacteria with the ability to degrade  $\text{ClO}_4^-$  immediately upon its addition (Section 3.1). Two main phyla, *Proteobacteria* and *Bacteroidetes*, were found before  $\text{ClO}_4^-$  addition to the reactor with relative amounts of 75.5% and 22.8%, respectively, and 60.5% and 28.2%, respectively, after the addition of  $\text{ClO}_4^-$ . Within the phylum *Proteobacteria*, only *Betaproteobacteria* was present, while the second phylum, *Bacteroidetes*, consisted of only *Flavobacteriia*.

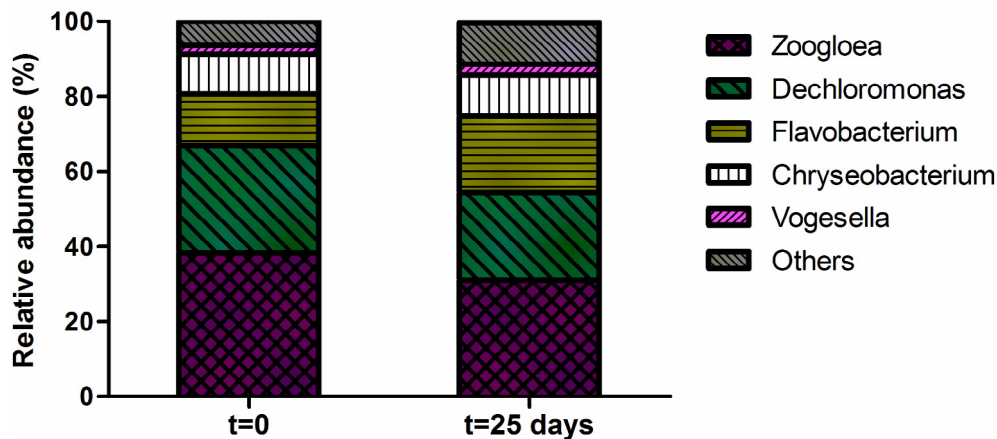


Fig. 3. Relative abundance of dominant genera in the pressurized hydrogenotrophic denitrifying reactor, before ( $t = 0$ ) and after ( $t = 25$  days) the addition of  $\text{ClO}_4^-$ .

Fig. 3 shows the relative amounts of the dominant genera before and after the addition of  $\text{ClO}_4^-$ . *Zoogloea* was the dominant genus in the reactor both before and after the addition of  $\text{ClO}_4^-$ , accounting for 38.3% and 31.0%, respectively, followed by *Dechloromonas* (28.7% before, 23.4% after), *Flavobacterium* (13.7% before, 20.3% after), *Chryseobacterium* (10.5% before, 11.0% after), and *Vogesella* (2.4% before, 2.9% after). Less significant genera are listed as 'Others' (6.4% before, 11.0% after). All five genera have species that can carry out denitrification, but only *Dechloromonas* has been associated with denitrification and  $\text{ClO}_4^-$  reduction [31].

PCR-DGGE analysis of the pressurized hydrogenotrophic denitrifying reactor gave similar results with seven nearly identical bands observed before and after the addition of  $\text{ClO}_4^-$  (Fig. 4). Four of the bands from the DGGE were sequenced (Fig. 4, Lane 1) and compared to the closest phylogenetic relatives found in the NCBI gene bank of the predominant bacteria recovered from high throughput sequencing (*Zoogloea ramigera*, *Zoogloea resiniphila*, *Dechloromonas hortensis*, *Dechloromonas agitata*, *Vogesella perlucida*, *Flavobacterium cheniae*, and *Chryseobacterium soli*). The aligned sequences from high throughput sequencing and PCR-DGGE are presented in Fig. 5.

The phylogenetic tree shows a divergence of only 5%, with DGGE bands-1,2 showing a near 100% similarity to *Dechloromonas* sp., while DGGE bands-3,4 have a close similarity with *Flavobacterium* and *Chryseobacterium*. The reactor's ability to metabolize  $\text{ClO}_4^-$  almost immediately from the outset of  $\text{ClO}_4^-$  addition was due to the large presence of *Dechloromonas* as confirmed by high throughput sequencing and PCR-DGGE analysis. Strains of *Dechloromonas* have been shown to grow on  $\text{ClO}_4^-$  and  $\text{NO}_3^-$ , while its ability to use  $\text{H}_2$  as an electron donor has also been shown [32]. Significant changes were not observed in the microbial population after 25 days of concurrent  $\text{ClO}_4^-$  and  $\text{NO}_3^-$  reduction, primarily due to the much greater electron accepting capacity (EAC) of  $\text{NO}_3^-$  (15 mg/L or 5.4 mequiv EAC) as opposed to  $\text{ClO}_4^-$  (20 mg/L or 1.6 mequiv EAC) during the experimental period.

### 3.3. Reduction of different electron acceptors in the combined treatment scheme

Following the initial investigation of  $\text{ClO}_4^-$  reduction using only the pressurized hydrogenotrophic reactor, the removal of different electron acceptors ( $\text{NO}_3^-$ -N,  $\text{NO}_2^-$ -N,  $\text{ClO}_4^-$  and  $\text{SO}_4^{2-}$ -S) was studied in the combined treatment scheme at different flow rates for two months. The inlet concentrations of  $\text{NO}_3^-$ -N and  $\text{ClO}_4^-$  were adjusted to 25 and 10 mg/L, respectively, while  $\text{SO}_4^{2-}$ -S concentrations in tap water ranged between 7 and 9 mg/L. The results are summarized in

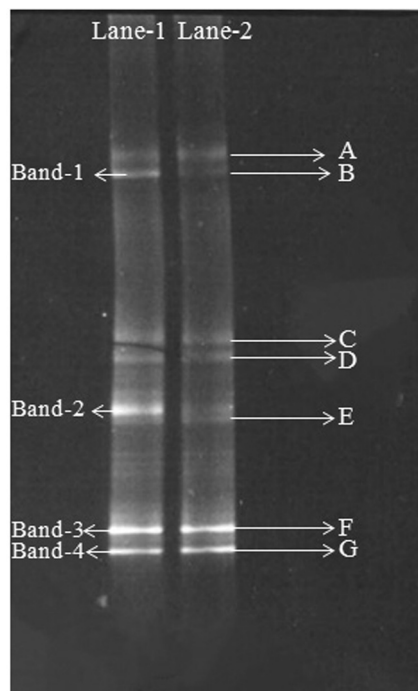


**Fig. 4.** PCR-DGGE analysis, Lane-1: pressurized hydrogenotrophic denitrifying reactor before the addition of  $\text{ClO}_4^-$ ; Lane-2: pressurized hydrogenotrophic denitrifying reactor after the addition of  $\text{ClO}_4^-$ . Dominant bands are labeled A to G. Bands 1, 2, 3 and 4 were sequenced.

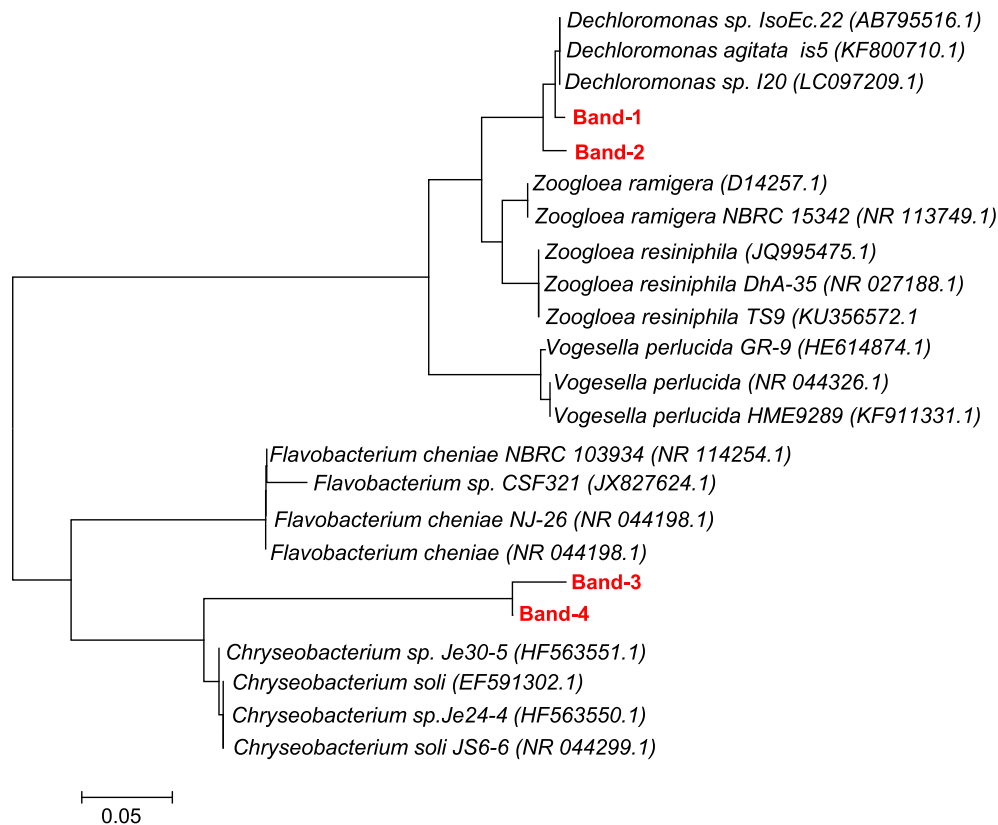


**Fig. 5.** Phylogenetic tree comparison of bacteria determined by high throughput sequencing and PCR-DGGE sequences (bands-1, 2, 3, 4) from the pressurized hydrogenotrophic denitrifying reactor.

**Fig. 6.** All measurements in Fig. 6 were repeated five times, each in a different day.

As expected, higher  $\text{NO}_3^-$ -N removal was observed in the main reactor unit at lower flow rates due to the higher retention time. Significant  $\text{ClO}_4^-$  removal was observed in the main reactor unit (from 10 to 2 mg/L) only when the lowest flow rate was applied; probably due to the higher retention time with the correspondent lower  $\text{NO}_3^-$ -N concentration (CSTR conditions, i.e.,  $\text{NO}_3^-$ -N concentration of about 1 mg/L). At higher flow rates, the effluent  $\text{NO}_3^-$  concentration in the main reactor increased and the average  $\text{ClO}_4^-$  removal rates calculated in the main reactor unit decreased (0.73, 0.3 and 0.26 g/(L<sub>reactor</sub>-d) for the operation with 150, 225 and 300 mL/min, respectively), suggesting that simultaneous removal of  $\text{NO}_3^-$  and  $\text{ClO}_4^-$  occurred with inhibition of  $\text{ClO}_4^-$  reduction due to the competition for electrons by  $\text{NO}_3^-$  [33].

In the polishing unit denitrification always occurred, while significant  $\text{ClO}_4^-$  reduction (>1 mg/L) occurred only in the presence of very low  $\text{NO}_3^-$ -N concentrations. Sulfate reduction was observed only in the presence of very low  $\text{NO}_3^-$ -N and  $\text{ClO}_4^-$  concentrations. These results can be explained by the combination of low concentration of dissolved  $\text{H}_2$  in the polishing unit (Section 3.4), higher denitrifying population than perchlorate-reducing population in the system,  $\text{NO}_3^-$  reduction by some perchlorate-reducing bacteria (Section 3.2) and the thermodynamics-based priority of  $\text{NO}_3^-$  and  $\text{ClO}_4^-$  reduction over  $\text{SO}_4^{2-}$  reduction. Therefore, further reduction of  $\text{ClO}_4^-$  to concentration close to zero occurred in the polishing unit only under the lowest flow rate when the  $\text{NO}_3^-$ -N concentration was already very low. The average  $\text{ClO}_4^-$  removal rates calculated in the polishing unit were much lower compared to the main reactor unit (0.12, 0.02 and 0 g/(L<sub>reactor</sub>-d) for the operation with 150, 225 and 300 mL/min, respectively). This observation

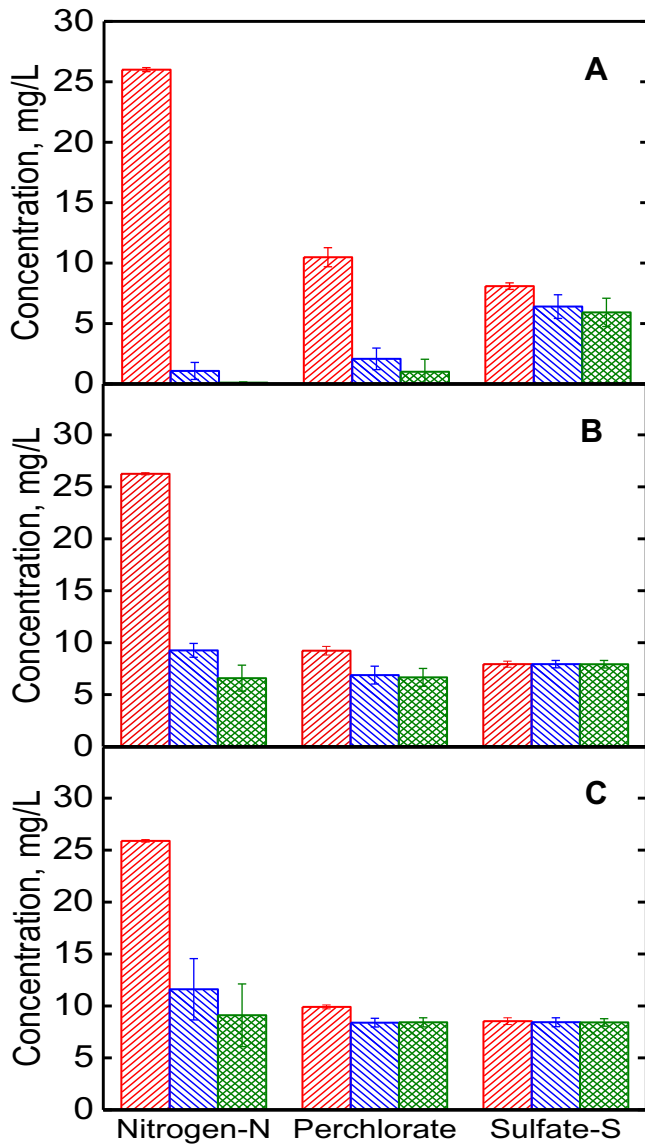


**Fig. 6.** Concentration of the inorganic nitrogen ( $\text{NO}_3^-$ -N +  $\text{NO}_2^-$ -N),  $\text{ClO}_4^-$  and  $\text{SO}_4^{2-}$ -S in the influent (red), effluent of the main reactor unit (blue) and effluent of the polishing unit (green) at different flow rates of (A) 150 mL/min; (B) 225 mL/min; and (C) 300 mL/min. (For interpretation of the references to colour in this figure legend, the reader is referred to the web version of this article.)

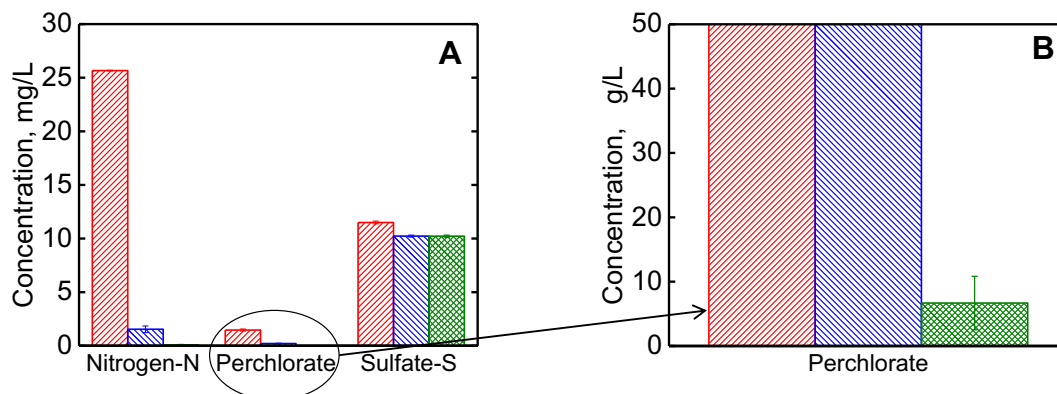


**Fig. 7.** Left (A): Concentration of the inorganic nitrogen ( $\text{NO}_3^-$ -N +  $\text{NO}_2^-$ -N),  $\text{ClO}_4^-$  and  $\text{SO}_4^{2-}$ -S in the influent (red), effluent of main reactor unit (blue) and effluent of polishing unit (green) at a flow rate of 155 mL/min. Right (B): zoom-in of the  $\text{ClO}_4^-$  column in units of  $\mu\text{g/L}$ . (For interpretation of the references to colour in this figure legend, the reader is referred to the web version of this article.)

can be attributed to the lower  $\text{ClO}_4^-$  concentration in the polishing unit. Also, the lower  $\text{NO}_3^-$  concentration in the polishing unit may not support a significant growth of  $\text{ClO}_4^-$  reducing bacteria as in the main reactor unit [8]. In the case where  $\text{NO}_3^-$  or  $\text{ClO}_4^-$  are further reduced in the polishing unit, an improved  $\text{H}_2$  utilization is achieved. Sulfate reduction is not one of the treatment goals and therefore does not improve  $\text{H}_2$  utilization in terms of financial aspects. However, it minimizes the amount of  $\text{H}_2$  released to atmosphere and therefore may contribute to the safety of the process. Detailed calculations and measurements for  $\text{H}_2$  utilization efficiencies are described in the next section. DOC analysis showed a minor increase of 0.15 mg/L after the polishing unit as compared to the inlet of the polishing unit.

#### 3.4. Hydrogen utilization and effluent quality using the combined system for the treatment of typical polluted groundwater

Following the experiments with relatively high influent  $\text{ClO}_4^-$  concentrations, the removal of a lower inlet  $\text{ClO}_4^-$  concentration of 1.5 mg/L (the  $\text{NO}_3^-$ -N concentration remained 25 mg/L) was studied in order to simulate typical conditions and to check the ability of the polishing unit to decrease  $\text{ClO}_4^-$  levels to trace concentrations, below 15  $\mu\text{g/L}$ . The flow rate in this experiment was adjusted to 155 mL/min.

The removal of  $\text{ClO}_4^-$ , together with that of  $\text{NO}_3^-$ -N and  $\text{SO}_4^{2-}$ -S, over the different treatment stages at steady state are shown in Fig. 7. Fig. 7 shows that  $\text{ClO}_4^-$  concentration was reduced to an average trace level of lower than 7  $\mu\text{g/L}$  in the polishing unit. The lowest value observed during steady state was 2  $\mu\text{g/L}$ . Together with reduction of  $\text{NO}_3^-$  and  $\text{NO}_2^-$  concentrations to below 0.1 mg/L, without any accumulation of chlorate ( $\text{ClO}_3^-$ ) and chlorite ( $\text{ClO}_2^-$ ), and with minimal increase in DOC concentration after the biological process (maximum DOC measured in effluent water was ~2 mg/L compared to 0.6 mg/L in feed water), the combined treatment scheme is suitable for drinking water production. The plug-flow character of the polishing unit is advantageous for reducing  $\text{ClO}_4^-$  concentrations to such low trace levels for two main reasons: (1) in CSTRs, reaching such low trace concentrations is harder due to mixing with the inlet stream having much higher concentrations; (2) better performance of  $\text{ClO}_4^-$  reduction can be achieved downstream after depletion of  $\text{NO}_3^-$ .

The submerged-flow regime in the polishing unit minimizes  $\text{H}_2$  discharge to the atmosphere and allows for its further consumption. In the polishing unit where  $\text{ClO}_4^-$  concentration is very low,  $\text{NO}_3^-$  can also support growth of  $\text{ClO}_4^-$  reducing bacteria and thus maintain this bacterial population [8]. Fig. 7 also shows that no

**Table 1**

Results achieved using the combined treatment scheme for the treatment of typical polluted groundwater (1.5 mg ClO<sub>4</sub><sup>-</sup>/L and 25 mg NO<sub>3</sub><sup>-</sup>-N/L).

Denitrification rate in main reactor unit [g N/(L <sub>reactor</sub> ·d)]	2.154 ± 0.028
Total pressure in main reactor unit [bar]	2.5
Theoretical H <sub>2</sub> pressure at steady-state in the main reactor unit [bar]	0.36
Measured H <sub>2</sub> pressure at steady-state in the main reactor unit [bar]	0.39 ± 0.01
Dissolved H <sub>2</sub> concentration in the effluent of the main reactor unit at saturation [mg/L]	0.59 ± 0.01
Measured dissolved H <sub>2</sub> concentration in the effluent of the main reactor unit [mg/L]	0.52 ± 0.04
H <sub>2</sub> utilization efficiency after the main reactor unit [%]	95.4 ± 0.3
Theoretical consumption of H <sub>2</sub> in the polishing unit [mg/L]	0.56
Measured dissolved H <sub>2</sub> concentration in the effluent of the polishing unit [mg/L]	0.002 ± 0.004
H <sub>2</sub> utilization efficiency after the polishing unit [%]	99.979

\* Based on Epsztein et al. [24].

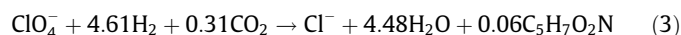
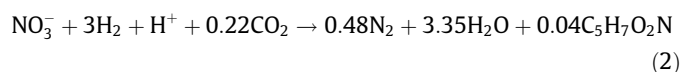
\*\* Using Henry's constant of 1.5 mg H<sub>2</sub>/(L·bar).

SO<sub>4</sub><sup>2-</sup> reduction was observed in the polishing unit due to the low concentrations of H<sub>2</sub> (Table 1).

Table 1 summarizes the main results and calculations at steady state, including GC analyses for H<sub>2</sub> concentration in gas and liquid phase. Table 1 shows the high denitrification rates obtained in the pressurized reactor as compared to other technologies, even at low effluent NO<sub>3</sub><sup>-</sup>-N concentrations. The rate can be further increased by applying higher recirculation rates [25]. A good correlation was found between measured and theoretical H<sub>2</sub> pressure in the closed-headspace reactor, indicating steady-state conditions. As expected, the measured dissolved H<sub>2</sub> concentration was a bit lower than its value at saturation due to H<sub>2</sub> consumption by biomass. The H<sub>2</sub> utilization efficiencies of the main pressurized reactor unit or the combined treatment scheme were calculated by Eq. (1).

$$H_2 \text{ utilization efficiency} = \frac{H_c}{H_c + H_e} \times 100\% \quad (1)$$

where  $H_e$  is the measured dissolved H<sub>2</sub> in the effluent of the main reactor unit or the polishing unit; and  $H_c$  is the H<sub>2</sub> consumption (in units of mg/l) in the main reactor unit or overall process. In order to calculate the H<sub>2</sub> consumption, a previously suggested metabolic stoichiometry for hydrogenotrophic denitrification [34] (Eq. (2)) and SO<sub>4</sub><sup>2-</sup> reduction [35] were used. For ClO<sub>4</sub><sup>-</sup> reduction, the metabolic stoichiometry (Eq. (3)) was built applying the same yield coefficient used for hydrogenotrophic denitrification due to the similar thermodynamics of the processes [10].



The H<sub>2</sub> utilization efficiency calculated after the main reactor unit was similar to the previous findings in the pressurized reactor [24]. The theoretical consumption of H<sub>2</sub> in the polishing unit was based on the assumption that all three electron acceptors were reduced by H<sub>2</sub> consuming bacteria. The result (0.56 mg/L) was very close to the measured dissolved H<sub>2</sub> after the main reactor unit (0.52 mg/L), albeit a bit higher. The difference can be attributed to minor heterotrophic activity. The almost zero residual of H<sub>2</sub> in the polishing unit effluent correlates well with the fact that SO<sub>4</sub><sup>2-</sup> was not reduced in the second unit due to lack of H<sub>2</sub>. The results of the combined treatment scheme show almost complete H<sub>2</sub> utilization with a total consumption of 10.9 mg H<sub>2</sub> per liter of water treated. To the best of our knowledge, our results of 100% utiliza-

tion of H<sub>2</sub> gas together with reduction of perchlorate concentration to low trace concentrations of ~2 μg/L were previously reported only for the MBfR [10].

#### 4. Conclusion

A new treatment scheme for removal of NO<sub>3</sub><sup>-</sup> and ClO<sub>4</sub><sup>-</sup> from drinking water, based on an unsaturated-flow pressurized hydrogenotrophic reactor combined with an up-flow submerged-bed open-to-atmosphere polishing unit was investigated. Degradation of ClO<sub>4</sub><sup>-</sup> started immediately after the addition of ClO<sub>4</sub><sup>-</sup> to the pressurized denitrification reactor, indicating that no special inoculum was needed for adjusting the reactor for ClO<sub>4</sub><sup>-</sup> reduction. This finding was supported by the large presence of the genus *Dechloromonas* in the reactor prior to the introduction of ClO<sub>4</sub><sup>-</sup>. Co-reduction of NO<sub>3</sub><sup>-</sup> and ClO<sub>4</sub><sup>-</sup> was observed in the pressurized reactor with significant inhibition in the ClO<sub>4</sub><sup>-</sup> reduction rate at higher NO<sub>3</sub><sup>-</sup> concentrations. The combination of submerged and plug-flow conditions in the polishing unit minimizes the discharge to atmosphere of the residual dissolved H<sub>2</sub> from the pressurized reactor and allows for the decrease of ClO<sub>4</sub><sup>-</sup> concentration to trace levels of 2 μg/L. The further consumption of H<sub>2</sub> in the polishing unit resulted in an increase in H<sub>2</sub> utilization efficiency from 95% to almost 100%.

#### Acknowledgements

We acknowledge the *Hydrogen Technologies Research Laboratory* in the Technion and Maccabi Carasso for his financial support.

#### References

- [1] C. Seidel, C. Groman, An assessment of the state of nitrate treatment alternatives – final report, Am. Water Work. Assoc. (2011).
- [2] P. Brandhuber, S. Clark, K. Morley, A review of perchlorate occurrence in public drinking water systems, J. Am. Water Work. Assoc. 101 (2009) 63–73.
- [3] R. Nativ, E.M. Adar, Soil and groundwater contamination the Ramat Hasharon area, Annual scientific report submitted to the water authority, Tel-Aviv, 2005.
- [4] W.E. Motzer, Perchlorate: problems, detections and solutions, Environ. Forensics 2 (2001) 301–311.
- [5] B.E. Logan, D. LaPoint, Treatment of perchlorate- and nitrate-contaminated groundwater in an autotrophic, gas phase, packed-bed bioreactor, Water Res. 36 (2002) 3647–3653, [http://dx.doi.org/10.1016/S0043-1354\(02\)00049-0](http://dx.doi.org/10.1016/S0043-1354(02)00049-0).
- [6] D.E. Kimbrough, P. Parekh, Occurrence and co-occurrence of perchlorate and nitrate in California drinking water sources, Am. Water Work. Assoc. 99 (2007) 126–132.
- [7] K.A. Karanasios, I.A. Vasiliadou, S. Pavlou, D.V. Vayenas, Hydrogenotrophic denitrification of potable water: a review, J. Hazard. Mater. 180 (2010) 20–37, <http://dx.doi.org/10.1016/j.jhazmat.2010.04.090>.
- [8] N. Bardiya, J.H. Bae, Dissimilatory perchlorate reduction: a review, Microbiol. Res. 166 (2011) 237–254, <http://dx.doi.org/10.1016/j.micres.2010.11.005>.
- [9] B.E. Logan, A review of chlorate- and perchlorate-respiring microorganisms, Bioremediat. J. 2 (1998) 69–79.
- [10] R. Nerenberg, B.E. Rittmann, I. Najm, Perchlorate reduction in hydrogen-based membrane-biofilm reactor, J. AWWA 94 (2002) 103–114.
- [11] F. Di Capua, S. Papirio, P.N.L. Lens, G. Esposito, Chemolithotrophic denitrification in biofilm reactors, Chem. Eng. J. 280 (2015) 643–657, <http://dx.doi.org/10.1016/j.cej.2015.05.131>.
- [12] K.C. Lee, B.E. Rittmann, Applying a novel autohydrogenotrophic hollow-fiber membrane biofilm reactor for denitrification of drinking water, Water Res. 36 (2002) 2040–2052, <http://www.ncbi.nlm.nih.gov/pubmed/12092579>.
- [13] B. Rezanian, J.A. Oleszkiewicz, N. Cicek, Hydrogen-dependent denitrification of water in an anaerobic submerged membrane bioreactor coupled with a novel hydrogen delivery system, Water Res. 41 (2007) 1074–1080, <http://dx.doi.org/10.1016/j.watres.2006.11.016>.
- [14] M. Prosnansky, Y. Sakakibara, M. Kuroda, High-rate denitrification and SS rejection by biofilm-electrode reactor (BER) combined with microfiltration, Water Res. 36 (2002) 4801–4810, <http://www.ncbi.nlm.nih.gov/pubmed/12448523>.
- [15] S. Xia, C. Wang, X. Xu, Y. Tang, Z. Wang, Z. Gu, Y. Zhou, Bioreduction of nitrate in a hydrogen-based membrane biofilm reactor using CO<sub>2</sub> for pH control and as carbon source, Chem. Eng. J. 276 (2015) 59–64, <http://dx.doi.org/10.1016/j.cej.2015.04.061>.
- [16] C. Zhu, H. Wang, Q. Yan, R. He, G. Zhang, Enhanced denitrification at biocathode facilitated with biohydrogen production in a three-chambered

- bioelectrochemical system (BES) reactor, *Chem. Eng. J.* 312 (2017) 360–366, <http://dx.doi.org/10.1016/j.cej.2016.11.152>.
- [17] Z. Wang, M. Gao, Y. Zhang, Z. She, Y. Ren, Z. Wang, C. Zhao, Perchlorate reduction by hydrogen autotrophic bacteria in a bioelectrochemical reactor, *J. Environ. Manage.* 142 (2014) 10–16, <http://dx.doi.org/10.1016/j.jenvman.2014.04.003>.
- [18] A.K. Sahu, T. Conneely, K. Nusslein, S.J. Ergas, Hydrogenotrophic denitrification and perchlorate reduction in ion exchange brines using membrane biofilm reactors, *Biotechnol. Bioeng.* 104 (2009) 483–491, <http://dx.doi.org/10.1002/bit.22414>.
- [19] M. Gao, S. Wang, Y. Ren, C. Jin, Z. She, Y. Zhao, S. Yang, L. Guo, J. Zhang, Z. Li, Simultaneous removal of perchlorate and nitrate in a combined reactor of sulfur autotrophy and electrochemical hydrogen autotrophy, *Chem. Eng. J.* 284 (2016) 1008–1016, <http://dx.doi.org/10.1016/j.cej.2015.09.082>.
- [20] C.T. Matos, S. Velizarov, J.G. Crespo, M.A.M. Reis, Simultaneous removal of perchlorate and nitrate from drinking water using the ion exchange membrane bioreactor concept, *Water Res.* 40 (2006) 231–240, <http://dx.doi.org/10.1016/j.watres.2005.10.022>.
- [21] H.P. Zhao, A.O. Valencia, Y. Tang, B.O. Kim, S. Vanginkel, D. Friese, R. Overstreet, J. Smith, P. Evans, R.K. Brown, B. Rittmann, Removal of multiple electron acceptors by pilot-scale, two-stage membrane biofilm reactors, *Water Res.* 54 (2014) 115–122.
- [22] X. Chen, Y. Liu, L. Peng, B.J. Ni, Perchlorate, nitrate, and sulfate reduction in hydrogen-based membrane biofilm reactor: Model-based evaluation, *Chem. Eng. J.* 316 (2017) 82–90, <http://dx.doi.org/10.1016/j.cej.2017.01.084>.
- [23] D. Friese, Demonstration and commercialization of ARoNite™, a novel hydrogen-based membrane biofilm biological reduction process, *Nitrate Treat. Technol. Work.* (2013). [http://ca-nv-awwa.org/canv/downloads/sessions/20/Session20\\_0800\\_Friese\\_Hills.pdf](http://ca-nv-awwa.org/canv/downloads/sessions/20/Session20_0800_Friese_Hills.pdf) (accessed December 27, 2016).
- [24] R. Epsztein, M. Beliaevski, S. Tarre, M. Green, High-rate hydrogenotrophic denitrification in a pressurized reactor, *Chem. Eng. J.* 286 (2016) 578–584, <http://dx.doi.org/10.1016/j.cej.2015.11.004>.
- [25] R. Epsztein, M. Beliaevski, S. Tarre, M. Green, Simplified model for hydrogenotrophic denitrification in an unsaturated-flow pressurized reactor, *Chem. Eng. J.* 306 (2016) 233–241.
- [26] C. Glass, J. Silverstein, Denitrification kinetics of high nitrate concentration water: pH effect on inhibition and nitrite accumulation, *Water Res.* 32 (1998) 831–839, [http://dx.doi.org/10.1016/S0043-1354\(97\)00260-1](http://dx.doi.org/10.1016/S0043-1354(97)00260-1).
- [27] B. Rezaia, N. Cicek, J.A. Oleszkiewicz, Kinetics of hydrogen-dependent denitrification under varying pH and temperature conditions, *Biotechnol. Bioeng.* 92 (2005) 900–906, <http://dx.doi.org/10.1002/bit.20664>.
- [28] G. Muyzer, E.C. De Waal, A.G. Uitterlinden, Profiling of complex microbial populations by denaturing gradient gel electrophoresis analysis of polymerase chain reaction-amplified genes coding for 16S rRNA, *Appl. Environ. Microbiol.* 59 (1993) 695–700.
- [29] C. Desitti, U. Cheruti, M. Beliaevski, S. Tarre, M. Green, Long-term atrazine degradation with microtube-encapsulated *Pseudomonas* sp. strain ADP, *Environ. Eng. Sci.* 33 (2016) 167–175.
- [30] K. Tamura, G. Stecher, D. Peterson, A. Filipski, S. Kumar, MEGA6: molecular evolutionary genetics analysis version 6.0, *Mol. Biol. Evol.* 30 (2013) 2725–2729.
- [31] M.A. Horn, J. Ihssen, C. Matthies, A. Schramm, G. Acker, H.L. Drake, *Dechloromonas denitrificans* sp. nov., *Flavobacterium denitrificans* sp. nov., *Paenibacillus anaericanus* sp. nov. and *Paenibacillus terrae* strain MH72, N<sub>2</sub>O-producing bacteria isolated from the gut of the earthworm *Aporrectodea caliginosa*, *Int. J. Syst. Evol. Microbiol.* 55 (2005) 1255–1265.
- [32] A.O. Valencia, C.R. Penton, R.K. Brown, B.E. Rittmann, Hydrogen-fed biofilm reactors reducing selenate and sulfate: community structure and capture of elemental selenium within the biofilm, *Biotechnol. Bioeng.* 113 (2016) 1736–1744.
- [33] H. Choi, J. Silverstein, Inhibition of perchlorate reduction by nitrate in a fixed biofilm reactor, *J. Hazard. Mater.* 159 (2008) 440–445, <http://dx.doi.org/10.1016/j.jhazmat.2008.02.038>.
- [34] P.L. McCarty, Stoichiometry of biological reactions, in: *Proc. Int. Conf. Toward a Unified Concept Biol. Waste Treat. Des.*, Atlanta, Georgia, 1972.
- [35] H.S. Van Wageningen, S.W. Söttemann, N.E. Ristow, M.C. Wentzel, G.A. Ekama, Development of a kinetic model for biological sulphate reduction with primary sewage sludge as substrate, *Water SA* 32 (2006) 619–626, <http://dx.doi.org/10.4314/wsa.v32i5.47833>.